P- ISSN 1991-8941 E-ISSN 2706-6703
2023,(17), (2):210– 224

Journal of University of Anbar for Pure Science (JUAPS)

Open Access

Antibacterial activity of NiTi alloy with sputtered tantalum

Seenaa Eesa Kadhim[1]*, Bilal K. Al-rawi [2], Mohammed K. Khalaf [3]

[1,2] Department of Physics, College of Education for Pure Sciences, University of Anbar, Iraq;
[3]Ministry of Science and Technology Material Research Directorate- Applied Physics, Iraq;

ARTICLE INFO

Received: 05 / 08 /2023
Accepted: 09 / 09 / 2023
Available online: 18 /12 / 2023

DOI: 10.37652/juaps.2023.142363.1109

Keywords:
Mactrontronic Sputtering Plasma Technology, Intelligent Nickel-Titanium (NiTi) Alloy, Tantalum Oxide, Optical Properties

ABSTRACT

A study was conducted on the use of the Mactrontronic Sputtering (DC) plasma technique by sprinkling tantalum metal (Ta) and depositing it on shape-memory nickel-titanium (NiTi) alloy and glass substrates in the presence of oxygen and argon gases. As a result, a coating of tantalum oxide (Ta_2O_5) deposited on the (NiTi) alloy was obtained. The change of the atomization plasma energy on the size of the precipitated oxide particles (Ta_2O_5) and its effect on the structural properties was discussed. For the membrane, the X-ray diffraction (XRD) tests showed that the films prepared at energies of (10, 15, 25, 30, and 35 watts) showed an amorphous structure, and the (AFM) results confirmed that the thinly deposited films consisted of spherical particles. Moreover, the results of the optical properties study showed the effect of annealing (heat treatment), whereby the annealing improved all the optical parameters of the deposited films. In addition, the contact angle measurements showed that the (Ta_2O_5) films exhibited hydrophilic characteristics and increased wettability for the (NiTi) alloy, which normally contributes to enhancing its resistance to bacteria and facilitating cell connection. Bacterial antimicrobial assays demonstrated that the deposited membrane exhibited antibacterial activity against both negative and positive bacteria. In particular, the test results revealed that the (NiTi) alloy samples coated with (Ta_2O_5) membrane had a higher bacteria-killing percentage for both negative and positive bacteria compared to the uncoated samples.

Introduction

Biomaterials are available in nature and can be manufactured to be used as implants or prosthetic parts as an alternative to joints in the human body. They have been used in the medical field on a large scale in the human body, including artificial heart valves [1], vascular stents, and alternative implants [2], such as shoulders, knee joints, and hips [3]. They were also used in dental implants [4]. In this context, thin coatings made of titanium and its alloys, which are called bioceramics, such as the (NiTi) medical alloy, have become the focus of recent research in the field of materials science, where bioceramics show suitable biological activity [5]. In this regard, the (NiTi) alloy has been used in biomaterials applications because the tantalum (Ti) and its alloys have promising mechanical properties and high biocompatibility.

These materials are recognized as standard materials for medical applications [6,7] due to their high biocompatibility since body cells can recognize (Ti) alloys, including (NiTi) [8]. The particles produced from erosion cause inflammatory reactions that inevitably lead to bone loss. Moreover, corrosion leads to the release of (Ni) ions of a toxic nature in the medical (NiTi) alloy, which affects the strength of the material and its biocompatibility due to fluid interactions in the human body. For this reason, we resorted to using tantalum to make a protective coating for the medical alloy (NiTi) for the purpose of improving its mechanical properties. In this regard, researchers found that tantalum(Ta) has good coating potential with mechanical properties similar to bone hardness and elasticity [9]. Then, tantalum was sprayed in the presence of the oxygen gas at a rate of (10%) and in the presence of an inert gas, such as argon, at a rate of (90%) to obtain the tantalum oxide (Ta_2O_5), which was deposited on the male-shaped (NiTi) alloy. More specifically, the tantalum

*Corresponding author at: Department of Physics, College of Education for Purs Sciences, University of Anbar, Iraq;
ORCID:https://orcid.org/0000-0002-0525-9172;Tel:+964000000
E-mail address: mohammedkhkh@yahoo.com

(Ta) was chosen because it reacts faster with the oxide compared to titanium (Ti), which leads to the adhesion of the coating to the surface [9]. Particularly, oxygenation with (Ta) gives a hard surface with high corrosion resistance [6], which is the aim of this study. After coating the (NiTi) alloy with a layer of (Ta_2O_5), the improvement of the mechanical properties of the (NiTi) alloy and its biocompatibility in medical applications is to be studied by conducting structural, optical, and mechanical examinations for specimens coated and uncoated with the tantalum oxide.

Materials and Methods

Utilizing the direct current (DC) plasma sputtering technology, with a gas mixture of 90% argon (Ar) and 10% oxygen (O_2) at a deposition pressure of (4×10^{-2}) Torr and a temperature range of (35°C) to (40°C) for a duration of two hours, the tantalum (Ta) was used as a coating target to improve the surface properties of the (NiTi) alloy substrate with a purity of 99.99%, a diameter of (5 cm), and a thickness of (4.5 cm). In particular, the (NiTi) alloy substrate was used as a base for deposition, and the distance between the target (Ta) and the substrate was (5 cm), with different sputtering powers of 10, 15, 25, 30, and 35 watts. Deposition substrates made of the (NiTi) alloy (Ni 54% - Ti 46%) with a purity of (99.99%) and glass slices were used. The (NiTi) alloy samples were cut into disks with a diameter of (2 cm) and a thickness of (2 mm), and then they were polished and smoothed. The disks were cleaned by washing them in distilled water and ethanol and then dried in an oven at (80°C) for at least half an hour. The samples were then introduced into a DC sputtering system with different sputtering powers. Next, the samples were analyzed using X-ray diffraction (XRD), atomic force microscopy (AFM), scanning electron microscopy (SEM), and energy-dispersive X-ray spectroscopy (EDX). Furthermore, the optical properties were examined using UV-Visible spectroscopy.

Results and discussion

1. X-ray diffraction

3-1- The X-ray Diffraction (XRD) Analysis

The X-ray diffraction of the tantalum film (Ta) deposited on bases of nickel-titalum alloys (NiTi) and bases of glass was investigated using the (DC) plasma technique, with different atomizing capacities of (30, 35, 25, 15, and 10 watts) and using the argon gas with a ratio of (10, 30, 25, and 35) (*Ar* 90%) and oxygen (O_2 10%). The results showed the growth of tantalum oxide films (Ta_2O5) on the metallic (NiTi) and the glass bases, which is due to the presence of oxygen gas inside the sedimentation system. From Figure (1), we note that the tantalum oxide films deposited on the glass bases have an amorphous structure as the results of the (XRD) examination showed a wide amorphous peak (Amorphase), and this is due to the crystalline nature of the tantalum oxide. These results are consistent with what has been found in some previous studies [10]. It is worth noticing that temperatures in the range (650-800 ℃) are required for the amorphous state, and since the temperature of the precipitate was less than (800 ℃), the amorphous interfacial films appeared, which is consistent with the results of the researchers in [11].

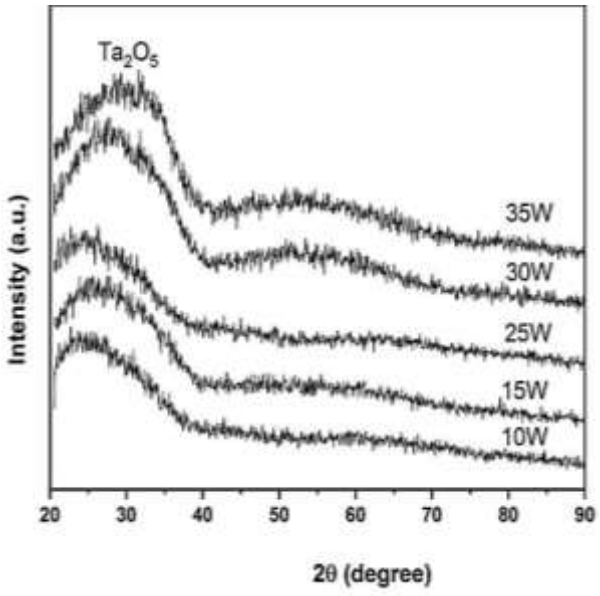

Figure 1. XRD patterns of (Ta_2O_5) films deposited on glass bases with atomized capacities of (10, 15, 25, 30, and 35 watts)

We also notice in Figure (1) that with the increase in the atomization power, especially at the power of (25 W), the intensity of the diffraction pattern begins to increase to the highest value, which can be compared with the international standard card (1199-21) (ICCD),

which represents (Ta_2O_5), and this is the result of increasing the precipitated atoms and thus increasing the thickness and crystallization of the prepared film. The increase in crystallinity of the films with the increase in atomizing ability is due to the improvement of the crystalline size and the decrease in the crystalline boundaries, which is consistent with the results of the researchers in [12].

From Figure (2), we notice that the (Ta_2O_5) film deposited on the glass substrates has an atomizing capacity of (15W), where the properties of the deposited film were studied before annealing at temperatures in the range (35 - 40 ℃) and after annealing at a temperature of (450 ℃) in a vacuum thermal oven. We also observe an increase in the uniformity of the deposited film through an increase in the intensity of the clear diffraction pattern.

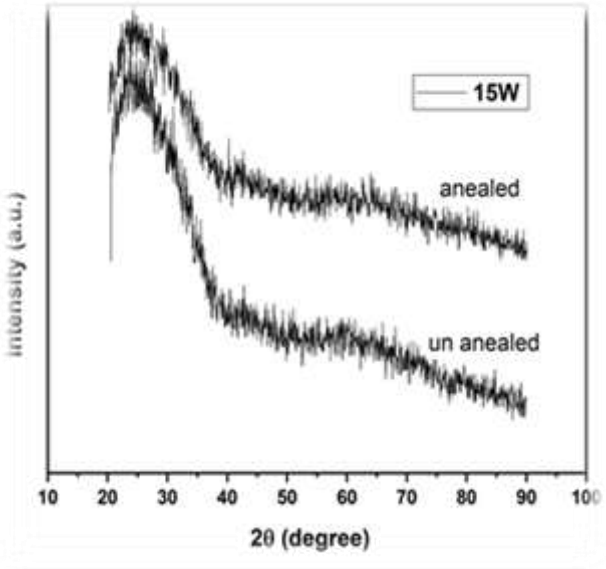

Figure 2. The XRD patterns of (Ta_2O_5) films deposited on glass substrates with (15W) atomization capacity before and after annealing at a temperature of (450 ℃).

Figure (3) shows the (Ta_2O_5) films deposited on the metal bases of the medical alloy (NiTi), where we can notice that it has a broad peak for the oxide (Ta_2O_5) in its amorphous form for the coated samples.

It was also observed that the (NiTi) alloy has crystalline levels appearing at angles 2θ of (42, 8-78, and 15) with (110) (211) crystal plane, which corresponds to the International Standard Card (1199-21) ICCD.

Moreover, it is evident from the comparison of the examination results for all samples that by increasing the atomizing ability, the crystallization of the (Ta_2O_5) membrane increases due to the amorphous nature of the (Ta_2O_5) membrane at temperatures less than (650 ℃), which is consistent with the results of the researchers in [11].

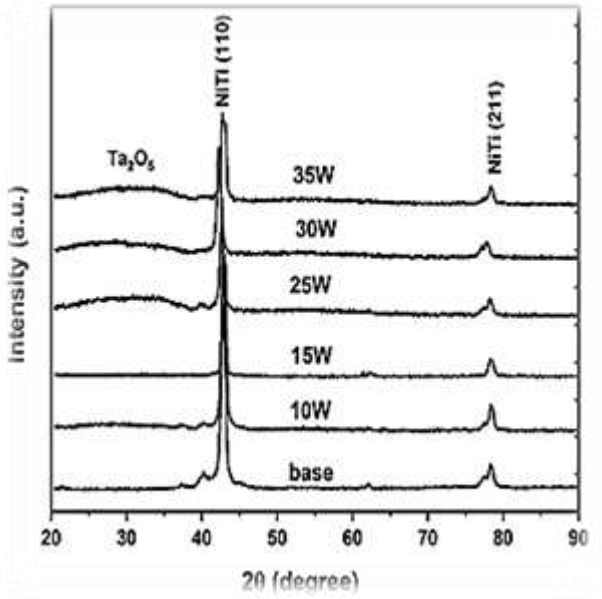

Figure 3. The XRD patterns of (Ta_2O_5) films deposited on metallic bases (NiTi alloy) with atomized capacities of (10, 15, 25, 30, and 35 watts) .

(3-2)Atomic Force Microscope (AFM) measurements:

From the AFM image analysis, we can calculate the surface roughness and the grain size. This analysis also gives an illustration of the distribution rate of the crystalline grain size on the surface. In particular, the films were deposited on glass bases with atomizing capacities of (35, 30, 25, 15, and 10 watts) and temperatures within the range of (35-40 ℃), and the results are shown in Table (1). In this regard, there is a noticeable change in the surface shape and roughness of the oxide films depending on the increase in the atomization energy of the plasma, where it can be observed that the rate of particle size decreases and the values of each of the mean square roots of the membrane change, which leads to a change in the value of the roughness rate of the deposited film since the increase in the energy of plasma atomization at a gas pressure of (10^{-2}) leads to an increase in the film thickness and a

decrease in the particle size, which causes a decrease in the size of the granules. Specifically, it can be noticed that the highest value of the particle size equals (86 *nm*) and the lowest thickness of the film equals (90.4 *nm*) at the atomizing power of (10 W), which is the lowest energy for the plasma. The lowest value of the particle size is (37.5 *nm*), the thickness of the film is (226 *nm*), and the atomization energy is (25 W), as shown in Figure (4) for the particle distribution, as there is an inverse proportion between the particle size and the increase in atomizing plasma energy in capacities of (25, 15, and 10 watts). As for the atomizing power of (30 and 35 watts) as illustrated in Figure (5), it is clear that the particle size started to increase due to the decrease in the thickness of the membrane caused by the phenomenon of re-sputtering that occurs with high atomizing energy, which is consistent with the results of the researchers in [13]. This result is due to the increase in the atomization energy, which leads to an increase in the sedimentation rate and, thus, a decrease in the time available for the sedimented particles to diffuse. Furthermore, the decreasing diffusion length of the sedimented particles hinders the growth of the particles inside the thin film, which reduces the particle size of the membrane and increases the energy of the atomizing plasma in capacities of (10, 15, and 25 watts), which is consistent with the results of the researchers in [14].

From the two-dimensional (2D) and the three-dimensional (3D) AFM images of the (Ta_2O_5) films, it can be observed that they contain light and dark areas of the color surfaces used to determine the vertical profile of the thin film surface, where the light areas represent the highest points and the dark points are the depressions. This figure confirms that the films are homogeneous and that the substrate surface is well-covered with almost uniformly distributed coatings. In addition, the 3D images reveal the presence of large sharp islands, which are formed by the deposited coating particles. The three-dimensional images also show that the surface of the deposited films showed a greater degree of roughness with an increase in the atomizing capacity, which indicates that the deposited surface increases its roughness with an increase in the atomizing energy. In other words, a surface with high biocompatibility can be obtained with an increase in the surface roughness and the atomizing energy, which is consistent with the results of the researchers in [15]. In addition, the average grain size of the root mean square (RMS) roughness can be observed, as shown in Table (1).

Table 1. The results of the atomic force microscopy measurement.

Sputtering Power / Watt	Thickness *nm*	Average Roughness *nm*	Root mean Square *nm*	Average Grain size
10	**90.4**	**2.890**	**4.198**	**86**
15	**130**	**9.465**	**13.408**	**44**
25	**226**	**3.163**	**4.5331**	**37.5**
30	**138.2**	**4.847**	**6.800**	**56**
35	**195.2**	**9.498**	**13.436**	**41**

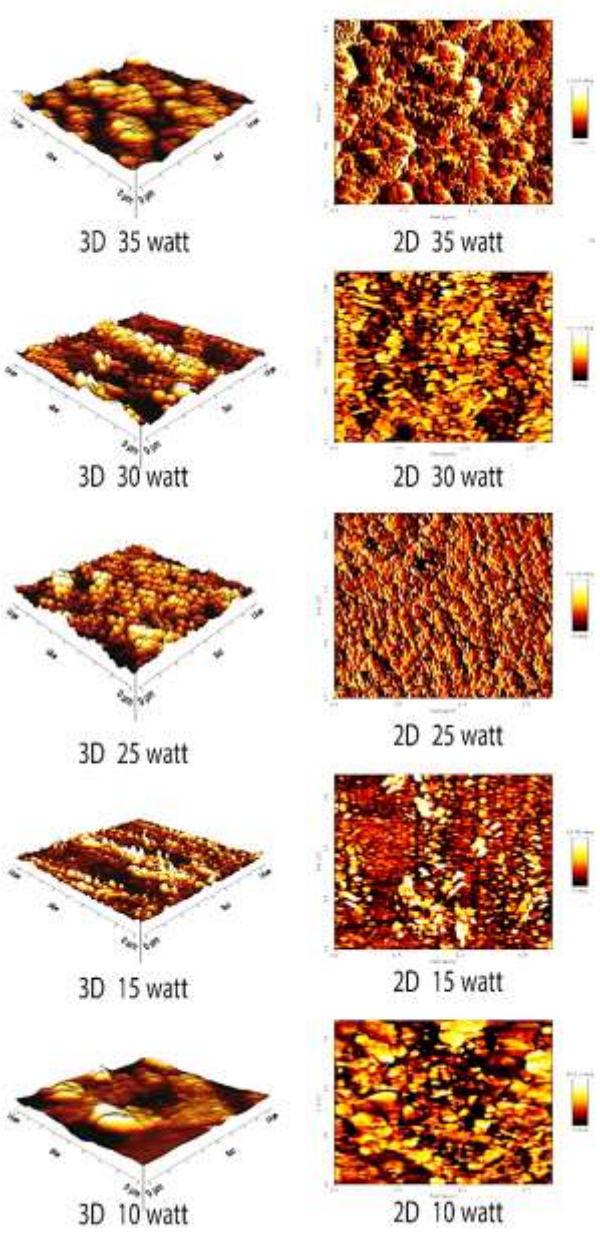

Figure 4. The (2D) and (3D) AFM microscopy images of the topography of the (Ta_2O_5) deposited films.

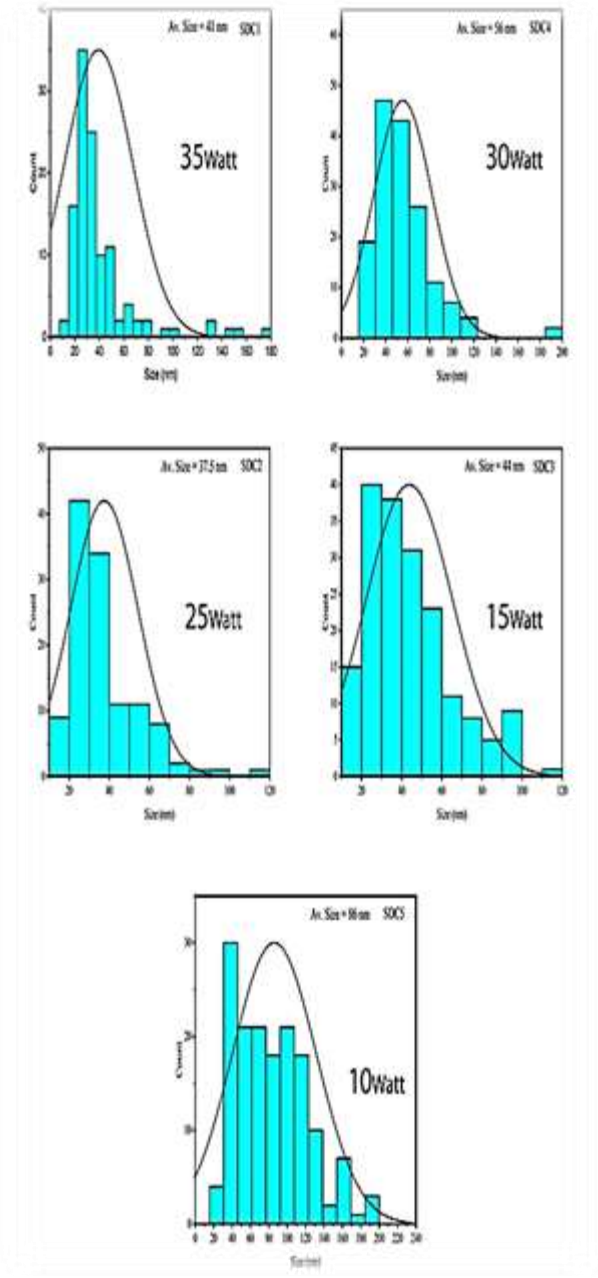

Figure 5. The granular distribution of the (Ta_2O_5) deposited films.

(3-3) Optical Properties:

The optical properties of the tantalum oxide films (Ta_2O_5) deposited on bases of glass were studied using the Macrontronian sputtering plasma technique and with atomizing capacities of (10-15-25-30-35 watts) through the transmittance and absorbance spectra within the positive length range of (300-1100 nm). The properties of the samples were measured before and after annealing. Then, the samples were heat-treated in a hot oven at (450 ℃) for one hour.

(3-3-1) Transmittance Spectra:

The surface nature, the material type, and the crystal structure determine the spectral transmittance of the thin films by calculating the algebraic sum of the transmittance (T), reflectivity (R), and absorbance (A). For those films, the nature of the transmittance spectrum of the (Ta_2O_5) films was identified. Figure (6) refers to the optical transmittance spectrum of the (Ta_2O_5) films with a wavelength range of (300 – 1100 nm) prepared with different atomizing capacities of (10 and 35 watts), where we notice in general that the intensity of the transmittance spectrum for the films deposited on glass bases and for all atomizing capacities increases with the increase in the wavelength. On the other hand, the transmittance is minimal at short wavelengths close to the region of (300 – 500 nm) as a result of the high absorption and electronic transitions. We also note from Figure (6) that the intensity of the transmittance spectrum for wavelengths shorter than 400 nm increases with the increase in the atomization capacity, especially for (25-35 watts), which is related to the increase in the thickness of the prepared films. This is due to the increase in the degree of crystallinity as a result of the high energies and the high temperature of the deposition bases, which agrees with the results of the researchers in [16]. The reason for this outcome is due to the increase in the number of atoms, which leads to an increase in the number of collisions between the falling atoms and the atoms of the membrane, where the crystalline nature of the membrane and the lattice arrangement of the atoms control the increase in absorption and the decrease in permeability, which is consistent with the results of the researchers in [17].

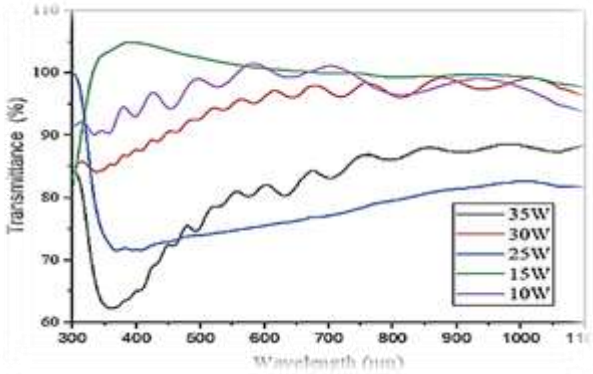

Figure 6. The transmittance spectrum as a function of the wavelength for the (Ta_2O_5) films prepared with different powers of (10-15-25-30-35 watts).

From Figures (7), (8), and (11), the intensity of the permeability spectrum of the annealed films (heat treated) is lower compared to that of the unplasticized films. This decrease is due to the diffusion of oxygen atoms within the crystalline structure and the creation of positional levels within the energy gap, which is consistent with the results of the researchers in [18, 19]. On the other hand, Figures (9) and (10) indicate that the intensity of the transmittance spectrum of the annealed films (heat treated) increases compared to that of the unplasticized films, and this is due to the increase in the degree of crystallinity of the membrane structures due to the increase in the grain size, which is consistent with the results of the researchers in [20].

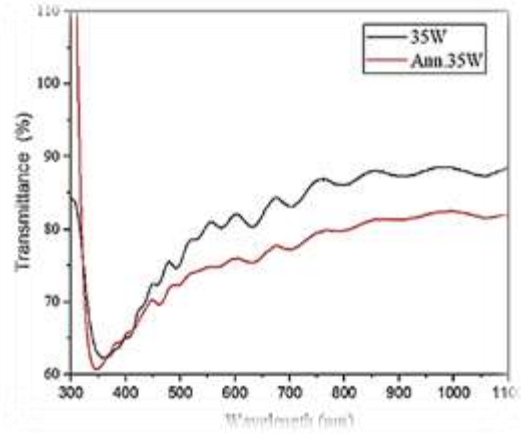

Figure 7. The transmittance spectrum of the (Ta_2O_5) film deposited on a glass base with an atomizing power of (35 watts) for the annealed and the un-annealed samples.

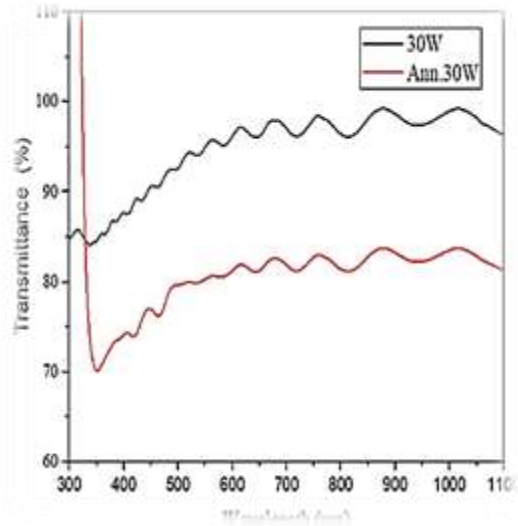

Figure 8. The transmittance spectrum of the (Ta_2O_5) film deposited on a glass base with an atomizing power of 30 watts for the annealed and the un-annealed samples.

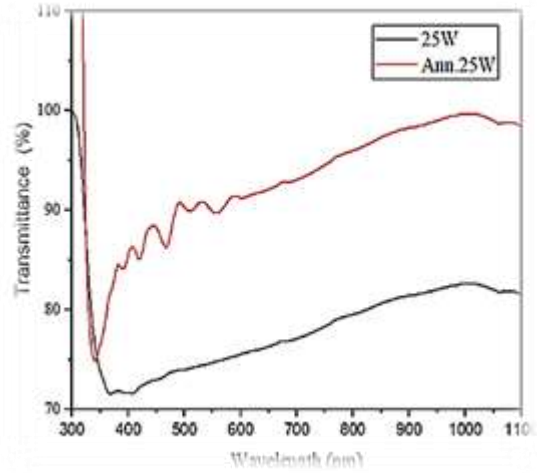

Figure 9. The transmittance spectrum of the (Ta_2O_5) film deposited on a glass base with an atomizing power (25 watts) for the annealed and the un-annealed samples.

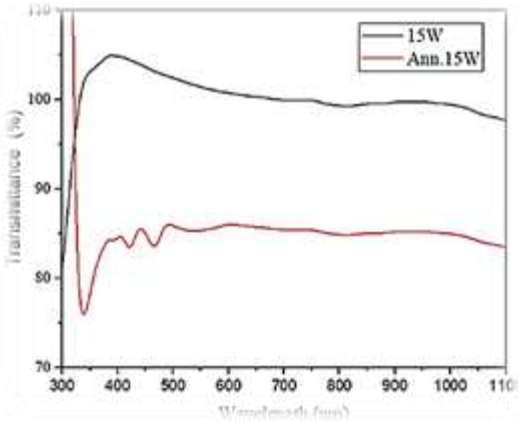

Figure 10. The tansmittance spectrum of the (Ta_2O_5) film deposited on a glass base with an atomizing power of (15 watts) for the annealed and the un-annealed samples.

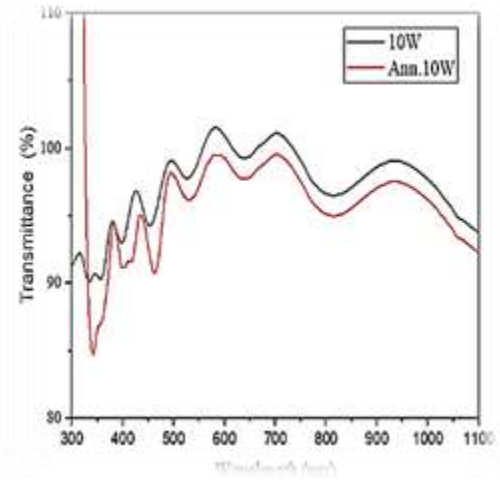

Figure 11. The transmittance spectrum of the (Ta_2O_5) film deposited on a glass base with an atomizing power of (10 watts) for the annealed and the un-annealed samples.

(2-3-3) Absorption Spectra:

Figure (12) depicts the absorbance curves as a function of the wavelength, which behave completely opposite to the transmittance curves, where it can be observed that the absorption curves increase with the decrease in the wavelength. The figure also shows that the absorbance increases with the increase in the atomizing power since the coated sample with the power of (35 watts) has a higher absorption rate than that of the coated sample with the power of (10 watts). The reason for the increase in the absorbance is due to the increase in the thickness of the coating, which is consistent with the results of the researchers in [21,22].

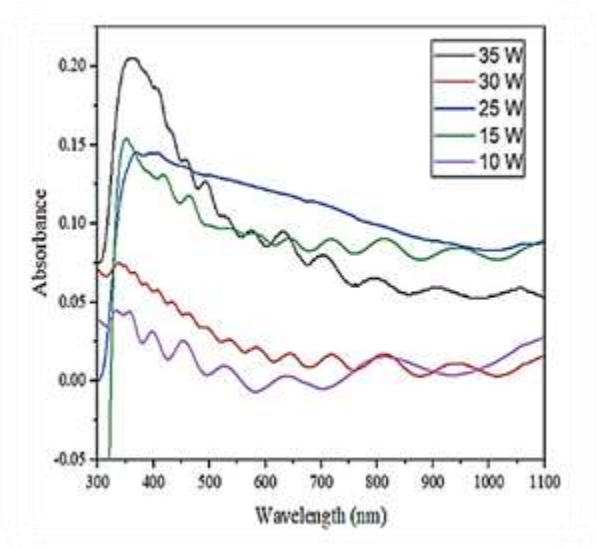

Figure 12. The absorbance spectrum as a function of the wavelength for the (Ta_2O_5) films prepared with different powers of (10-15-25-30-35 watts).

The main role of the absorption of thin films at wavelengths of (300-1100 nm) is located at the absorption edge. Therefore, the increase in the atomization power and the related change in the intensity of the absorption spectrum, as shown in Figures (12), (13), and (14), generally lead to a decrease in the intensity of the spectrum, especially at wavelengths shorter than (500 nm), which is attributed to a decrease in crystalline defects and an increase in the grain size with an increase in the deposition temperature, which is consistent with the results of the researchers in [23].

Figures (13) and (15) show the effect of heat treatment (annealing) on the absorption spectrum, and here it can be attributed to the high absorption of the tantalum oxide layer (Ta_2O_5) formed as a result of oxygen atoms and impurities interacting with tantalum atoms (Ta), which are spread within the energy gap for the prepared membranes. Figures (16) and (17) show the change in the intensity of the absorbance spectrum with the change in the wavelength of the annealed (heat-treated) and un-annealed samples. We note, as was previously explained, that the absorbance is the inverse of the permeability spectrum. Therefore, the heat treatment increases the crystallization of the thin films and thus decreases the crystalline defects and impurities within the energy gap. In other words, it decreases the intensity of the absorbance spectrum, which is consistent with the results of the researchers in [20].

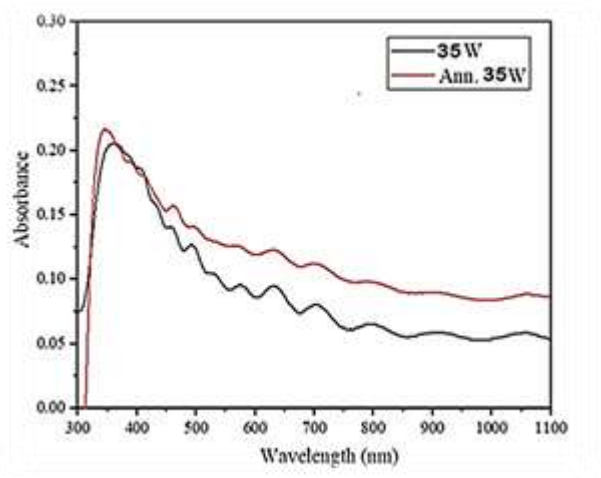

Figure 13. The absorption spectrum of the (Ta_2O_5) film deposited on a glass base with the atomizing power of (35 watts) for the annealed and the un-annealed samples.

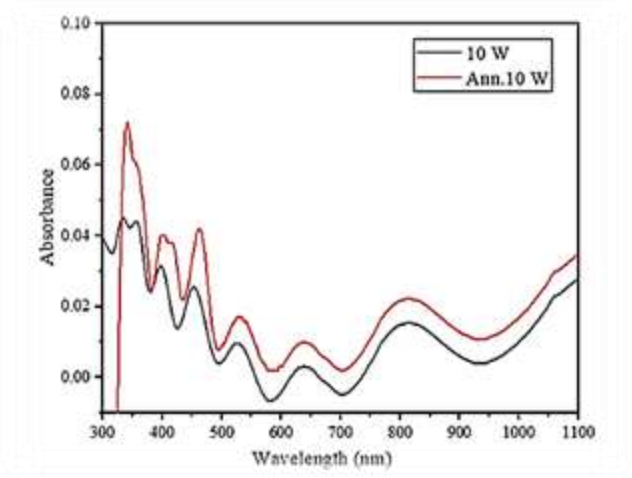

Figure 14. The absorption spectrum of the (Ta_2O_5) film deposited on a glass base with the atomizing power of (10 watts) for the annealed and the un-annealed samples.

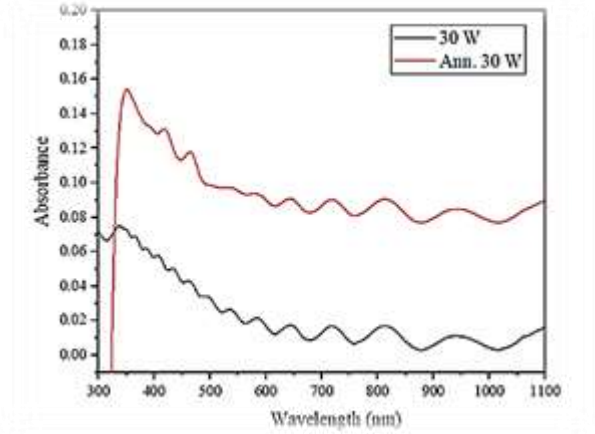

Figure 15. The absorption spectrum of the (Ta_2O_5) film deposited on a glass base with the atomizing power of (30 watts) for the annealed and the un-annealed samples.

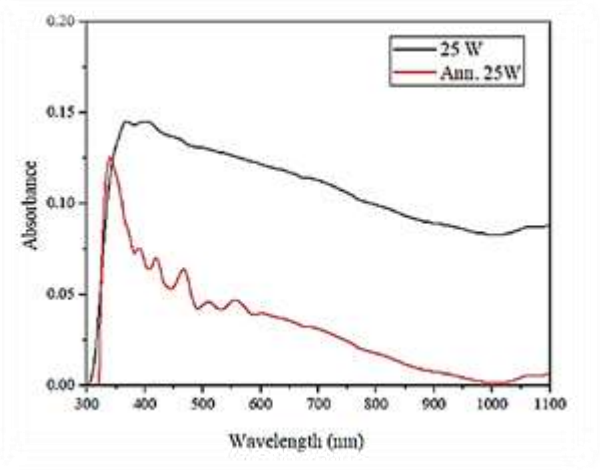

Figure 16. The absorption spectrum of the (Ta_2O_5) film deposited on a glass base with the atomizing power of (25 watts) for the annealed and the un-annealed samples.

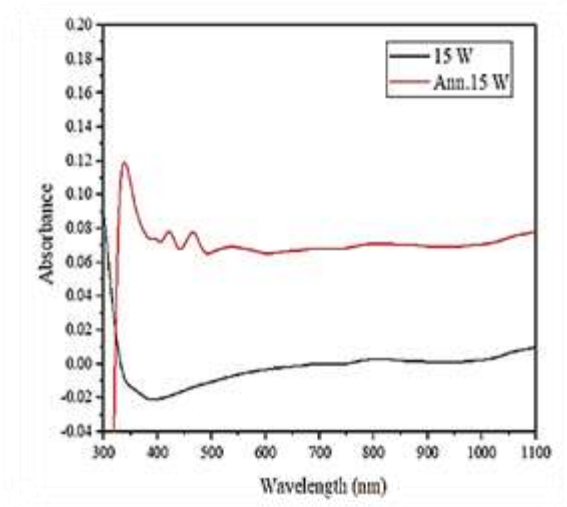

Figure 17. The absorption spectrum of the (Ta_2O_5) film deposited on a glass base with the atomizing power of (15 watts) for the annealed and the un-annealed samples.

(3-3-3) Optical Energy Gap

The energy gap is defined as the forbidden region for the presence of charge carriers within it, and the energy gap (eV) refers to the energy difference between the top of the valence band and the bottom of the conduction band in insulators and semiconductors, that is, it is the energy required to upgrade an electron from the valence band to the conduction band, which is consistent with the results of the researchers in [24]. The optical energy gap is considered one of the important constants since it gives a clear idea of the optical absorption. In particular, the energy gap (Eg) is affected by the type of prepared membrane and the precipitation method. In addition, the energy gap (Eg) is affected by the conditions of preparation and the structure nature of the prepared films, which is consistent with the results of the researchers in [25]. Specifically, the energy gap was determined from the visual image of the graphical relationship between photon energy (hv) on the x-axis and (αhv^2) on the y-axis. The extension of the straight line from the resulting curve will cut the x-axis (hv) at a certain point that represents the optical energy gap (Eg) for these films. From Table (2), it can be seen that the energy gap decreases with the increase in the atomizing energy, i.e., it decreases with the increase in the thickness of the deposited film. It can be observed that at the power gap is (10 W), the thickness is (90.4 nm), the energy gap is (3.17 ev), the energy gap measured at the atomizing power is (30 W), and the thickness is (138.2 nm). Moreover, for the power of (35W) and the thickness of (195.2nm), it was (2.50 eV). Therefore, the energy gap decreases with the increase in the density of the local states with the increase in thickness, which results in a decrease in the energy gap, which is consistent with the results of the researchers in [26], and the increase in the density of states is caused by defects due to the presence of oxygen in the deposited tantalum oxide films that works to create local levels within the energy structure, which is consistent with the results of the researchers in [19].

Figures (18), (19), (20), and (21) for the atomizing powers of (35, 30, 25, and 15), respectively, show a comparison of the energy gap of the samples before and after annealing at (450 ℃) for an hour.

We notice that the energy gap has increased after annealing, as shown in Table (2), and the reason is attributed to the improvement in the crystalline structure of the thin films after annealing, which is consistent with the results of the researchers in [21,27].

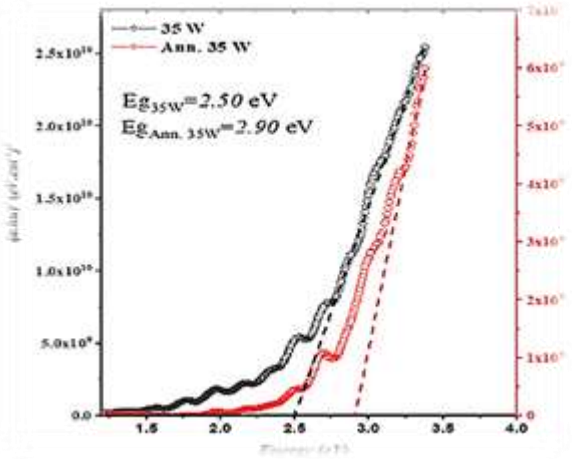

Figure 18. The energy gap of the (Ta_2O_5) film deposited on a glass base with an atomizing power of (35W) for the annealed and the un-annealed samples.

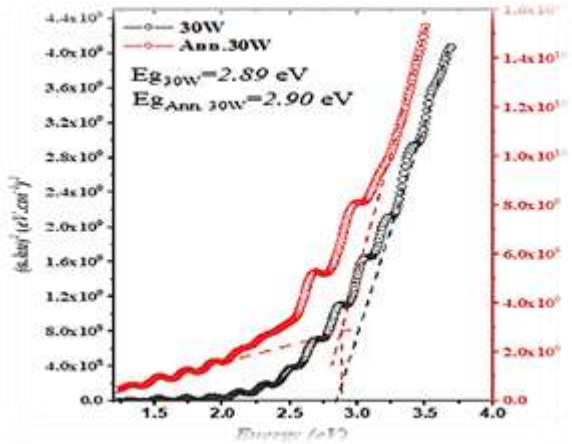

Figure 19. The energy gap of the (Ta_2O_5) film deposited on a glass base with an atomizing power o (30W) for the annealed and the un-annealed samples.

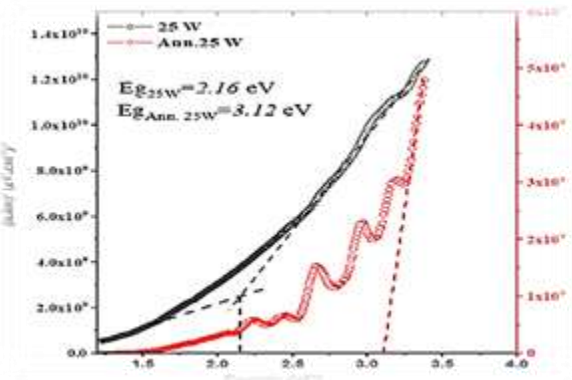

Figure 20. The energy gap of the (Ta_2O_5) film deposited on a glass base with an atomizing power of (25 W) for the annealed and the un-annealed samples.

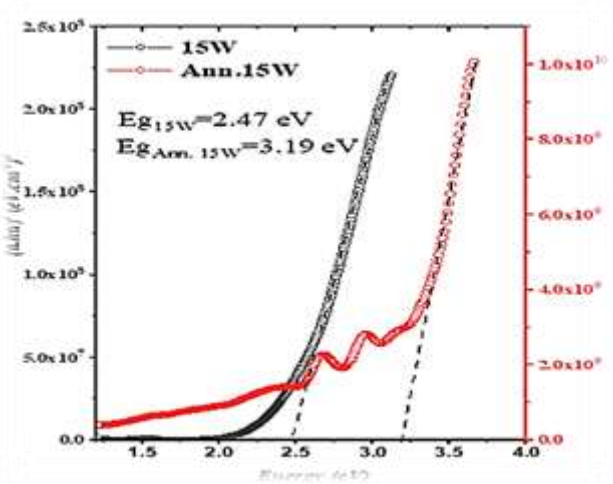

Figure 21. The energy gap of the (Ta_2O_5) film deposited on a glass base with an atomizing power of (15 W) for the annealed and the un-annealed samples.

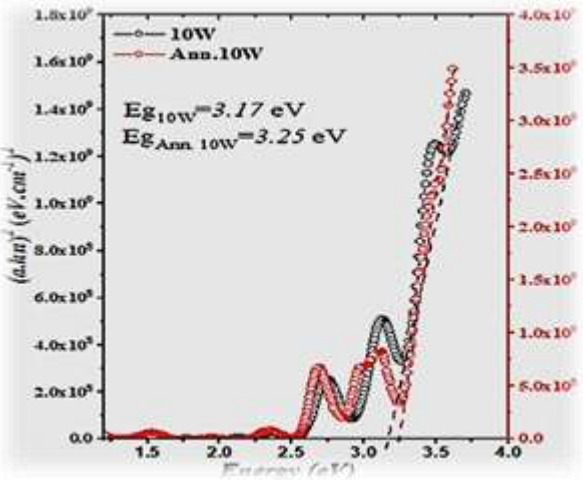

Figure 22. The energy gap of the (Ta_2O_5) film deposited on a glass base with an atomizing power of (10W) for the annealed and the un-annealed samples.

(3-3-4) Absorption Coefficient:

The optical absorption coefficient takes an important role in the optical calculations, as it varies with different materials and is a function of the wavelength of the incident light and affects the amount of light absorbed by the membrane. We note from Table (2) that the absorption coefficient increases with the increase in the thickness of the membrane, which is proportional to the increase in the blasting energy as well. Moreover, we note from the same table that the absorption coefficient also increases by an amount after

annealing, which is consistent with the results of the researchers in [28].

(3-3-5) Reflectance Spectra:

The reflectivity (*R*) is the ratio between the intensity of the reflected radiation to the intensity of the incident radiation. The reflectivity can be calculated depending on the transmittance and absorption spectra, as shown below [29]:

R + T + A = 1 ……(1)

R = reflectivity, T = transmittance, A = absorbance

From Table (2), we note that the reflectivity increases with the increase in the sputtering energy, that is, with the increase in the thickness of the dinner (Ta_2O_5).

(3-3-6) Refractive Index:

The refractive index (n) is the ratio between the speed of light in a vacuum to its speed inside a substance. The refractive index has been calculated for the (Ta_2O_5) films deposited on bases of glass with atomizing capacities of (10, 15, 25, 30, and 35 watts). It was found that the refractive index increases with the increase in the atomizing energy, that is, with the increase in the thickness of the film (Ta_2O_5).

(3-3-7) Extinction Coefficient:

The passivation coefficient (k) represents the attenuation of the electromagnetic wave that propagates through the material, where its value is estimated depending on the density of free electrons and the structural nature of the material. In this regard, we notice an increase in the damping coefficient with an increase in the atomization energy, i.e. with an increase in the thickness of the deposited film.

(3-3-8) Optical Dielectric Constant:

The interaction between the light and the charges of the medium is due to the absorption of energy in the material and then the process of polarization (polarization) of the charges of that medium, where the dielectric constant of its two types, real (ε_r) and imaginary $(\varepsilon)_i$, for membranes of (Ta_2O_5) was calculated. From table (2), we notice an increase in the value of the real dielectric constant (ε_r) and the imaginary dielectric constant $(\varepsilon)_i$ with an increase in the atomization energy, that is, with an increase in the thickness of the deposited film, which is the transmittance of the prepared films, which is consistent with the results of the researchers in [28].

Table 2. The optical properties of the (Ta_2O_5) film before and after annealing and with atomizing powers of (10-15-25-30-35 watts).

No	Power (Watt)	Thickness (nm)	State	absorption coefficient □ $(cm)^{-1}$	inertia coefficient K	refractive coefficient n	The real dielectric constant is ε_r	imaginary dielectric constant ε_i	Reflectivity R	Eg Gop eV
1	10	90.4		-1418.6	-0.006	Num#	Num#	Num#	-0.008	3.17
			Ann	21954.2	0.06	1.76	3.12	0.24	0.101	3.25
2	15	130		734.6	0.003	1.39	1.95	0.06	0.027	2.27
			Ann	2763.6	0.012	1.28	1.64	0.031	0.015	3.19
3	25	226		21945'2	0.096	1.93	3.7	0.37	0.101	2.16
			Ann	10824.1	0.046	1.61	2.60	0.153	0.055	3.12
4	30	138.2		5117.2	0.22	1.39	1.95	0.06	0.027	2.89
			Ann	21945.2	0.096	1.93	3.71	0.37	0.101	2.90
5	35	195.2		214179	0.099	1.91	3.66	0.35	0.099	2.50
			ANN	29132.9	0.127	2.09	4.36	0.53	0.126	2.90

4-Measuring the Contact Angle (θ):

The contact angle examination was carried out for the (NiTi) alloy samples coated and uncoated with titanium oxide (Ta_2O_5) with different atomizing capacities, using a drop of distilled water at the room temperature of (25 ℃). The test results showed that the coating of (Ta_2O_5) has contributed to the increase in the wettability of the (NiTi) alloy, because the contact angle measurement for the uncoated (NiTi) samples was (88.13-88.20) and the contact angle measurement for the coated (NiTi) samples ranged between (79.94-80.88), as shown in Figure (23).

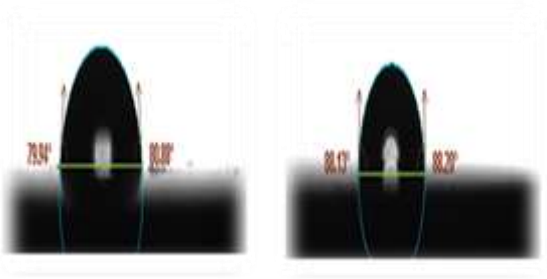

A **B**

Figure 23. The contact angle of the coated and the uncoated samples of the (NiTi) alloy, (a) the contact angle of the uncoated sample (b) the contact angle of the coated sample.

This means that the contact angle has decreased by (8.19-7.32 degrees), as shown in Table (4-11), which means that the surface of the (NiTi) alloy coated with (Ta_2O_5) is a hydrophilic surface because the angle is less than (90 degrees), which is consistent with the results of the researchers in [30].

The hydrophilic materials with contact angle ($\theta < 90$) have the ability to resist bacteria and facilitate cell and tissue bonding with the medical alloy. These features make oxide-coated (NiTi) (Ta_2O_5) suitable for biomedical engineering applications including prosthetic implants and they work as surgical implants inside the human body, which is consistent with the results of the researchers in [31,32].

5- Antibacterial Activity Test:

The antibacterial activity of the uncoated (NiTi) alloy and the tantalum oxide coated (NiTi) alloy (Ta_2O_5) was investigated using E.Coli grams negative and (S.tabhlococcus aureus-grams positive) [33].

In particular, about (20 ml) of Mold-Hinton (M H) agar was poured into sterile dishes, and bacterial species were collected from cultures stored using a sterile wire loop which is consistent with the results of the researchers in [34]. After cultivating and activating the bacteria, holes with a diameter of (6 mm) were drilled on the agar plates using a sterile tip, and the coated and uncoated samples were placed in a plastic container and placed in an incubator for 24 hours at a temperature of (37 ℃), after which the average diameter of the inhibition zones was recorded [35,36]. As shown in Figure (24), the sample coated with the tantalum oxide that was placed in the agar with gram-positive bacteria had greater antibacterial activity than that of the uncoated sample, as the inhibition rate for the coated sample was (31) and for the uncoated sample was (27), as shown in Table (3).

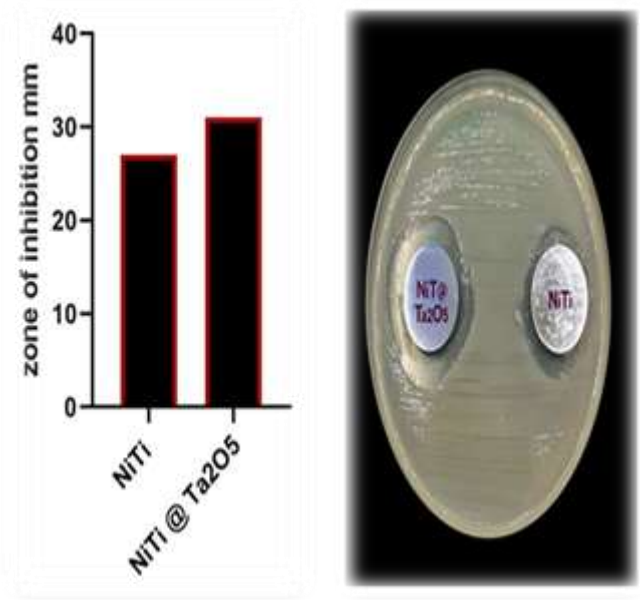

Figure 24. Antibacterial activity of (Ta_2O_5) and uncoated (Ta_2O_5) alloy against Staphylococcus aureus (Gram positive).

From Figure (25), we also notice that the samples coated with the tantalum oxide have antibacterial activity against gram-negative bacteria. Therefore, the inhibition rate for the coated sample was (25.5) and that for the uncoated sample was (19.5), as shown in Table (3), which indicates that the coating is (Ta_2O_5) improving the resistance properties of the (NiTi) alloy against bacteria and preventing the growth of (E.Coli) (S.aureuse). This improvement increases the

biocompatibility of the alloy and makes it safe in the manufacture of implants, medical devices, and equipment, which is consistent with the results of the researchers in[35,36].

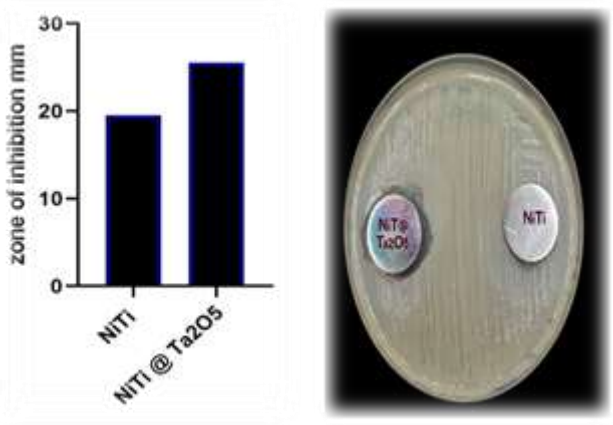

Figure 25. Antibacterial activity of (Ta_2O_5) and uncoated (Ta_2O_5) antibacterial activity against Escherichia coli (Gram-negative).

Table 3. The antibacterial activity of (Ta_2O_5) and uncoated (Ta_2O_5) alloy.

Samples		Zone of inhibition
S.aureus	NiTi	27
	Ta_2O_5 / NiTi	31
E.coli	NiTi	19.5
	NiTi / Ta_2O_5	25.5

Conclusion:

The results of this research confirmed that the change in the amount of atomization plasma energy can control the thickness of the film and the particle size of nanoparticles deposited on the (NiTi) shape-memory alloy and the glass substrates. The X-ray diffraction (XRD) measurements revealed a broad, amorphous peak of the as-deposited (Ta_2O_5) films. The study of the optical properties showed that the (Ta_2O_5) films have energy gaps whose values change in the range (2.6 eV - 3.17 eV) depending on the thickness of the deposited film. It was also found that all optical properties increase with the increase in the thickness of the deposited film except for the transmittance, and this was also found after the annealing procedure for the coated and the uncoated samples. Coated in a hot oven at (450 ℃) for an hour, it was found that the annealing improved all the optical properties of the deposited films. The results of the contact angle examination showed that the (Ta_2O_5) films have hydrophilic surfaces and have a high inhibition capacity for both gram-positive and gram-negative bacteria by comparing the bacteria-killing percentage between the coated and the uncoated samples with the tantalum oxide. Thus, it is clear that the (Ta_2O_5) oxide coating has improved the properties of the (NiTi) shape memory alloy, making it suitable to be used in medical applications, such as surgical implants or as medical tools and equipment.

References:

[1]G.J. Wilson Acellular matrix: a biomaterials approach for coronary artery bypass and heart valve replacement Ann. Thorac. Surg. (1995) https://doi.org/10.1016/0003-4975(95)98967-Y

[2] Z. Ma Surface engineering of electrospun polyethylene terephthalate (PET) nanofibers towards development of a new material for blood vessel engineering Biomaterials (2005) https://doi.org/10.1016/j.biomaterials.2004.07.026

[3] B. Sharma et al. Microstructure and properties of beta Ti–Nb alloy prepared by powder metallurgy route using titanium hydride powder J. Alloys Compd. (2016) https://doi.org/10.1016/j.jallcom.2015.10.053

[4] H. Farnoush Modification of electrophoretically deposited nano-hydroxyapatite coatings by wire brushing on Ti–6Al–4V substrates Ceram. Int. (2012) https://doi.org/10.1016/j.ceramint.2012.02.079

[5] Y.-M. Lim Functionally graded Ti/HAP coatings on Ti–6Al–4V obtained by chemical solution deposition Ceram. Int. (2002) https://doi.org/10.1016/S0272-8842(01)00055-4

[6] T.R. Rautray et al. Ion implantation of titanium based biomaterials Prog. Mater. Sci (2011) https://doi.org/10.1016/j.pmatsci.2011.03.002

[7] L. Nie Novel β-type Zr–Mo–Ti alloys for biological hard tissue replacements Mater. Des. (2014) https://doi.org/10.1016/j.matdes.2013.07.008

[8] N.T.C. Oliveira et al. Electrochemical stability and corrosion resistance of Ti–Mo alloys for biomedical applications Acta Biomater. (2009) https://doi.org/10.1016/j.actbio.2008.07.010

[9] B. Rahmati et al Ceramic tantalum oxide thin film coating to enhance the corrosion and wear

characteristics of Ti-6Al-4V alloy J. Alloys Compd (2016) https://doi.org/10.1016/j.jallcom.2016.03.188

[10] M.S.Mattsson, G.A.Niklasson .K.Forsgren , And A.Harsta , " A Frequency Yesponse And Transient Current Study Of B-Ta2o5: Methods Of Estimating The Dielectric Constant, Direct Currect Conduct Ivity , And Ion Mobility , J.Appl , Phys.85, 2185-2191(1999). https://doi.org/10.1063/1.369525

[11] Sanjan Sathasivam , Benjamin A.D.Williamson , Andreas kafizas , shaeel A. ALthabaiti , Abdullahy , obaid . sulaiman N.Basahel , DavidO , Scanlon , Claire J. car malt and ivan p. parkin . " A computational and experimental study of Ta2O5 Thin Films. https://doi.org/10.1021/acs.jpcc.6b11073

[12] Zhi – yue Li, Sheng-chichen , Qiu Hong Huo Ming – Hang Liao , ming – Jiang Dai , Song-Sheng Lin , Tian – Linyang and Huisun , " Influence of sputtering power on the electrical properties of In-Sn-Zn oxide thin films deposited by high power impuls magnetron sputtering" , coatings , 2019 . 9 (1 1) ,715.

[13] Bouer, W. Betz, G.Bangert,H.Bergauer, A., Eisenmenger Sttner, C:Intrin Sic Re-Sputtering During Film Depostin Investing Ated By Monte Carlo Simulation .J.Vac.Sci, Technol, A12 (6), 3157-3164(1994). https://doi.org/10.1116/1.579231

[14] Mf Cergueiraq, M Andritschky,L.Rebouta,Ja Ferreira And M.F Da Silva , "Microcrystalline Silicon Thin Films Prepared By Rf Reactive Magnetron Sputter Deposition (1995).

[15] Sidika Mine Toker , Gabriella Sugerma Elliot Christion Frey "Effect Of Surface Characteristies On The In Vitor Biocompatibility Response Of NiTi Shape Memory Alloys .(2019). https://doi.org/10.21541/apjes.461169

[16] Sharma R.S, Shukla R.K. And Kumar A., "Effect Of Ag Impurity On Photo Conductive Properties Of Selenium –Tellurium Glasses" . Journal Ovonic Research , Vol .3.No .6 (2007) Pp1 19-127.

[17] Al.Jamal Y.N. "Solid State Physics" , Al-Mosel University , (2 nd Ed) Arabic Version (2000) .hattps:// doi.org/10.1088/1742-6596/1999/1/012128

[18] P.Nemec, M.Frumar , B,Frumarov, M.Jelinek, J.Lancok , J.Jedelsky, Opt . Mater, 15(2000) 191, And Papers Cited Therein. https://doi.org/10.1016/S0925-3467(00)00035-5

[19] Mohammed khammas kalaf, " fabrication of pbse photo conductive detector and studying the effect of annealing time on its electro – optical properties , 1998.

[20] S.Rajagopalan , K.S.Hor Shvardh I .K.Mal Hotra, K.I. Chopra , J.NonCryst .Solids .50 (1982) 29.

[21] Obadia Amer Abdulhussein , Sami Salman Chiad Chiad , Nadir Fadhil Habubi, "Effect Of Poly Styrene Film Thickness On Some Optical Parameters". 881

[22] Haleh Kangarlou And Saeid Rafiza Deh. " Influence Of Thichness On Structural And Optical Properties Of Titanium Oxid Thin Layers .Www.Intech.Open.Com .

[23] J.M.R.AL-Obeadi , (2012), " studying the effect of thicknesson the structural and optical properties for zinc oxide impure by cd" university of Anbar MSC.

[24] Babu , V.Suresh ."Soild State Devices And Technology". (2010), 3 rd Edition. Peason.

[25] D.P.Padiyan ,A.Marikani , K.R.Murali , Physica B,357, 485 (2005). https://doi.org/10.1016/j.physb.2004.12.016

[26] M.A.Barote, A.A.Yadav,L.P Deshmukh , E. U. Masumdar , (Synhe Sis And Charactrrizatton Of Chemic Ally Deposted Cd × Pb × Thin Films . " (2010).

[27] Atheer M.Mkhaiber And Ameer. F.Abdulameer " The Effect Of Heat Treatment On The Optical Properties Od Organic Semiconductor (Nipc/C60) Thin Films. (2018).

[28] Kadhim A.Aadim , Ali A-K.Hussain , Mohammed R.Abdulameer, "Effect of annealing temperature and laser pulse energy on the optical properties of cuo films prepared by pulsed laser deposition" , 2014.

[29] O. Stenzel, ―The Physics of Thin Film Optical Spectra‖ ISBN: 09315195, Springer-Verlag Berlin Heidelberg, Germany, (2005).

[30] K. K. Chanab , B.Sohrabi , A.Rahman Zaden Biomater . Sci . 2019 , 7, 3 1 10.

[31] K. Liu, M.Cao , A.Fujishima , L.Jiang ,Chem .Rev . 2014 , 1 14 , 10044. https://doi.org/10.1021/cr4006796

[32] Y. Yuan,T.Randall. Contact Angle And Wething Properties , In G.Bracco.

[33] James B.kaper , James p.Nataro and Harry L.T.Mobley. " pathogenic Escherichia coil" , Nature Reviews Microbiology. 2,123-140 , 2004.

[34] Khansa K.S., Badr , B.A.,Sulaiman. G.M.,Jabir, M.S., and HUSSAIN s.a. (2021) , Antibacterial activity of zinc oxide nanostructured materials synthesis ny laser ablation method . in journal of physics: conference series (vol.1795, no.1 , p.012040)

[35] Jihad, M. A., Noori, F. T., Jabir, M. S., Albukhaty, S., AlMalki, F. A., & Alyamani, A. A. (2021). Polyethylene glycol functionalized graphene oxide nanoparticles loaded with nigella sativa extract: a smart antibacterial therapeutic drug delivery system. Molecules, 26(1 1), 3067. https://doi.org/10.3390/molecules26113067

[36] Mohammed, M.K., Mohammad, M.R., Jabir, M.S., and AHMED, D.S (2020) , Functionalization characterization and antibacterial activity of single wall and multi wall carbon nanotubes. In IOP Conference series: Materials Science and Engineering (vol.757, No.1 , p.012028). https://doi.org/10.47750/jptcp.2023.30.13.032

النشاط المضاد للبكتيريا لسبائك NiTi مع التنتالوم المرذذ

سيناء عيسى كاظم[1] بلال كمال الراوي[2] محمد خماس خلف[3]

[2،1]قسم الفيزياء، كلية التربية للعلوم الصرفة، جامعة الانبار، الانبار، العراق

[3]وزارة العلوم والتكنولوجيا مديرية أبحاث المواد – الفيزياء التطبيقية، العراق

mohammedkhkh@yahoo.com sc.bilal_alrawi@uoanbar.edu.iq san21u3008@uoanbar.edu.iq

الخلاصة:

تم اجراء دراسة حول استخدام تقنية بلازما الترذيذ الماكنتروني ,(DC) من خلال ترذيذ معدن التنتالوم (Ta) وترسيبة على ركائز من سبيكة النيكل تيتانيوم (NiTi) المتذكرة الشكل وركائز زجاجية، بوجود غاز الاوكسجين والاركون. تم الحصول على طلاء أوكسيد التنتالوم (Ta_2O_5) المترسب على سبيكة(NiTi). تمت مناقشة تغيير مقدار طاقة بلازما الترذيذ على حجم الحبيبات المترسبة من أوكسيد (Ta_2O_5) وتاثيرها ايضا على الخصائص التركيبة. للغشاء، حيث اظهرت فحوصات حيود الاشعة السينية (XRD) ان الاغشية التي تم تحضيرها عند الطاقات (10,15,25,30,35 W) اظهرت تراكيب ببنية غير متبلورة، كما اكدت نتائج (AFM) ان الاغشية الرقيقة المترسبة تتكون من جسيمات كروية. واظهرت نتائج دراسة الخصائص البصرية اثر التلدين (المعالجة الحرارية)، حيث عمل التلدين على تحسين جميع المعلمات البصرية للأغشية المترسبة. وأظهرت فحوصات زاوية التلامس(Contact Angle) أن أغشية (Ta_2O_5) هي من الأغشية المحبة للماء وقد أسهمت في زيادة التبللية (Wettability) لسبيكة (NiTi) مما يزيد من مقاومتها للبكتيريا وتسهيل ارتباط الخلايا. وأظهرت فحوصات النشاط المضاد للبكتيريا المرضية بنوعيها السالبة والموجبة أن الغشاء المترسب يمتلك نشاطا مضادا للبكتيريا، وقد أظهرت نتائج الفحص أن عينات سبيكة (NiTi) المطلية بغشاء (Ta_2O_5) تمتلك نسبة قتل للبكتيريا السالبة والموجبة أكبر من العينات غير المطلية.

الكلمات المفتاحية: تقنية بلازما الترذيذ الماكنتروني، سبيكة (NiTi) الذكية، أكسيد التنتالوم، الخصائص البصرية.